

HASNAS: A Hardware-Aware Spiking Neural Architecture Search Framework for Neuromorphic Compute-in-Memory Systems

Rachmad Vidya Wicaksana Putra, Muhammad Shafique
New York University (NYU) Abu Dhabi, Abu Dhabi, United Arab Emirates
{rachmad.putra,muhammad.shafique}@nyu.edu

ABSTRACT

Spiking Neural Networks (SNNs) have shown capabilities for solving diverse machine learning tasks with ultra-low-power/energy computation. To further improve the performance and efficiency of SNN inference, the Compute-in-Memory (CIM) paradigm with emerging device technologies such as resistive random access memory is employed. However, most of SNN architectures are developed without considering constraints from the application and the underlying CIM hardware (e.g., memory, area, latency, and energy consumption). Moreover, most of SNN designs are derived from the Artificial Neural Networks, whose network operations are different from SNNs. These limitations hinder SNNs from reaching their full potential in accuracy and efficiency. Toward this, we propose *HASNAS*, a novel hardware-aware spiking neural architecture search (NAS) framework for neuromorphic CIM systems that finds an SNN that offers high accuracy under the given memory, area, latency, and energy constraints. To achieve this, *HASNAS* employs the following key steps: (1) optimizing SNN operations to achieve high accuracy, (2) developing an SNN architecture that facilitates an effective learning process, and (3) devising a systematic hardware-aware search algorithm to meet the constraints. The experimental results show that our *HASNAS* quickly finds an SNN that maintains high accuracy compared to the state-of-the-art by up to 11x speed-up, and meets the given constraints: 4×10^6 parameters of memory, 100mm^2 of area, 400ms of latency, and $120 \mu\text{J}$ energy consumption for CIFAR10 and CIFAR100; while the state-of-the-art fails to meet the constraints. In this manner, our *HASNAS* can enable efficient design automation for providing high-performance and energy-efficient neuromorphic CIM systems for diverse applications.

1 INTRODUCTION

Recent advancements in neuromorphic computing have demonstrated the SNN capabilities for solving diverse machine learning (ML)-based applications with ultra-low-power/energy computation. Therefore, many studies have been performed to maximize SNN potentials in terms of algorithmic performance and efficiency, ranging from SNN developments [16, 24, 38], hardware accelerators [1, 5, 9], and deployments for diverse application use-cases, such as image classification [34, 39], object recognition for automotive [8], bio-signal processing for healthcare [20], continual learning for mobile systems [2, 35, 36], and embodied intelligence for robotics [4, 33].

In reality, different ML-based applications have different requirements of algorithmic performance (e.g., accuracy) and efficiency (e.g., latency and energy consumption). To ensure their practicality for real-world implementation, they also need to meet the constraints from the underlying hardware platforms (e.g., memory footprint and area). Therefore, *to maximize the SNN benefits for diverse application use-cases, SNN models have to be designed to fulfill the targeted accuracy and efficiency, while meeting the given constraints*, which is a non-trivial problem. For instance, a larger SNN model is usually employed to achieve higher accuracy, but it

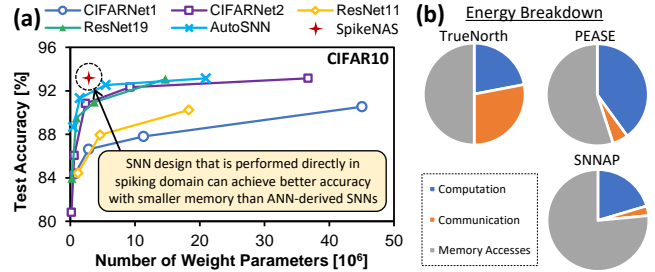


Figure 1: (a) Accuracy vs. memory footprint of different SNNs considering the CIFAR10 workload: CIFARNet1 [46], CIFARNet2 [12], ResNet11 [18], ResNet19 [48], AutoSNN [24], and SpikeNAS [38]; adapted from studies in [24, 38]. (b) Breakdown of energy consumption for SNN processing on different von Neumann-based neuromorphic hardware platforms: TrueNorth [1], PEASE [40], and SNNAP [42]; adapted from studies in [17].

leads to higher energy consumption as the memory accesses dominate the overall SNN processing energy in the von Neumann-based neuromorphic hardware platforms; see Fig. 1(a)-(b).

To substantially improve the efficiency of SNN processing, the non-von Neumann Compute-in-Memory (CIM) paradigm is employed [3, 23]. The CIM paradigm coupled with non-volatile device technologies, such as resistive random access memory (RRAM), overcomes the “memory wall bottleneck” by minimizing the data movements between memory and compute engine. However, simply running the existing SNN on a CIM platform may not satisfy the design requirements for the targeted application (e.g., in terms of accuracy, memory, area, latency, and energy consumption), since SNN models are typically developed without considering the characteristics of the CIM hardware. Moreover, most of SNN architectures are derived from conventional Artificial Neural Networks (ANNs), which have different operations from SNNs [24], hence they may lose unique features of SNN computation models (e.g., temporal information) that leads to sub-optimal accuracy [16]. Studies in [16, 38] show that designing an SNN architecture directly in the spiking domain can achieve better accuracy than deriving from the ANN domain; see Fig. 1(a). Therefore, *SNNs should be designed directly in a spiking domain to meet design requirements and constraints from the targeted application and underlying CIM hardware*. However, manually developing the suitable SNN architecture is time consuming and laborious, thereby requiring an alternative technique that can find a desired solution efficiently.

Research Problem: *How to automatically and quickly find an SNN architecture for neuromorphic CIM systems that achieves high accuracy and high efficiency (for latency and energy consumption) under memory and area constraints.* An efficient solution to this problem will ease the developments of high-performance and energy-efficient neuromorphic CIM systems, and enable their applicability for diverse ML-based applications.

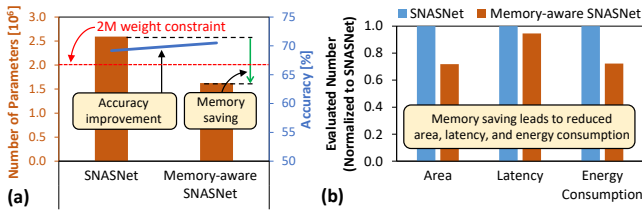


Figure 2: Results of the experimental case study considering SNASNet [16] and memory-aware SNASNet with the CIFAR100 workload: (a) number of weight parameters and the accuracy; (b) area, latency, and energy consumption when running the networks on an RRAM-based CIM platform [23].

1.1 State-of-the-Art and Their Limitations

Currently, state-of-the-art still focus on employing neural architecture search (NAS) for finding SNN architectures that offer high accuracy. They can be classified into the following categories.

- **NAS with training:** This approach employs “train-and-search” process, as it first trains a super-network that consists of all possible architecture candidates, and then searches a subset architecture that achieves target accuracy. It is employed by [24, 47]. *Limitations:* This approach typically incurs huge searching time, memory, and energy consumption.
- **NAS without training:** This approach addresses limitations of “NAS with training”. Its idea is to explore the architecture candidates using a building block/cell that represents network operations and topology, evaluates the fitness score of the investigated architecture, then trains the one with the highest score. *Limitations:* SNASNet employs a random search whose effectiveness relies on the number of iteration, and does not consider the processing hardware [16]. MSE-NAS employs a set of complex excitation-inhibition connectivity, and also does not consider the processing hardware [27]. AutoST and AutoSpikeformer only target spiking transformer architectures [7, 44]. LitESNN employs a complex topology and compression, and only considers memory cost in its NAS [19]. Meanwhile, SpikeNAS employs optimized network operations and considers memory cost in its NAS [38].

In summary, *the state-of-the-art NAS works for SNNs do not consider multiple design requirements and constraints posed by the targeted application and the CIM hardware platform (i.e., memory, area, latency, and energy consumption)*, thereby hindering the applicability of neuromorphic CIM systems for diverse ML-based applications. To demonstrate the limitations of state-of-the-art and highlight the optimization potentials, an experimental case study is performed and discussed in Section 1.2.

1.2 Case Study and Research Challenges

We study the benefits of applying constraints in the NAS through experiments. To do this, we reproduce the state-of-the-art Cell-Based NAS without training (i.e., SNASNet [16]), then we apply a memory constraint on it to build a memory-aware SNASNet. Here, we consider a constraint of 2×10^6 (2M) parameters for the CIFAR100 workload. We also consider a RRAM-based CIM platform [23] as the underlying processing hardware. Note, the details of Cell-Based NAS are discussed in Section 2.3, and the details of experimental setup are discussed in Section 4. Fig. 2 presents our experimental results, from which we have the following key observations.

- A smaller network may achieve comparable or better accuracy to the bigger network, meaning that there is a possibility to maintain high accuracy with a smaller network size.
- Memory saving leads to reduced area, latency, and energy consumption of SNN processing on an RRAM-based CIM platform.

These observations expose several research challenges that need to be addressed for solving the targeted research problem, as discussed in the following.

- The solution should quickly yet effectively perform its searching process to minimize the searching time.
- The solution should incorporate multiple design constraints (i.e., memory, area, latency and energy consumption) into its search algorithm to ensure the practicality of SNN deployment on the CIM platform.

1.3 Our Novel Contributions

To address the research challenges, we propose *HASNAS*, a novel Hardware-Aware Spiking NAS framework which quickly finds the SNN architecture that can achieve high accuracy under the given design requirements and constraints (i.e., memory, area, latency, and energy consumption) for realizing high-performance and energy-efficient neuromorphic CIM systems. This work is also the first work that develops an integrated hardware-aware spiking NAS for CIM systems. Our HASNAS employs several key steps as the following (as shown in Fig. 3).

- **Optimization of SNN Operations:** It aims to investigate SNN operations that can lead to high accuracy, while considering their memory costs. Then, the selected operations will be utilized for building the network architecture.
- **Development of Network Architectures:** It aims to build a network architecture that can facilitate effective learning process, by leveraging the selected SNN operations and carefully arranging the neural cell architectures.
- **A Hardware-aware Search Algorithm:** It aims to find a network architecture that can achieve high accuracy, by searching for suitable cell architectures, while monitoring the memory, area, latency, and energy consumption costs.

Key Results: We evaluate our HASNAS framework using a PyTorch-based implementation, and run it on an Nvidia RTX 4090 GPU machine. For constraints of 4M parameters of memory, $100mm^2$ of area, 400ms of latency, and $120\mu J$ of energy consumption, our HASNAS can quickly find an appropriate SNN with high accuracy comparable to the state-of-the-art by up to 11x speed-up on CIFAR10 and CIFAR100; while the state-of-the-art cannot meet the latency and energy constraints.

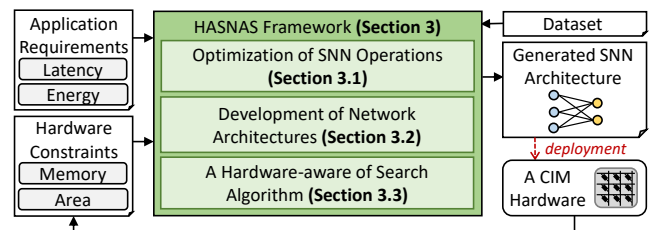


Figure 3: Overview of our novel contributions in the HASNAS framework; highlighted in green.

2 PRELIMINARIES

2.1 Spiking Neural Networks (SNNs)

SNNs are the neural networks' computational model that takes inspiration from how brain works, especially on how spikes are utilized for conveying information and data processing [21, 28, 41, 43]. SNN operations mainly rely on the neuronal dynamics, which vary depending on the neuron model. Typically, SNNs employ a leaky integrate-and-fire (LIF) neuron model, as it can provide diverse spike train patterns with a relatively low-complexity computation [14, 15]. The neuronal dynamics of LIF neuron model can be characterized with the following equations.

$$U_{mem}(t) = \lambda U_{mem}(t-1) + Y(t) \quad (1)$$

$$Y(t) = \sum_i w_i \delta_i(t) \quad (2)$$

$$Z(t) = \begin{cases} 1, & \text{if } U_{mem} \geq U_{thr} \\ 0, & \text{if otherwise} \end{cases} \quad (3)$$

Here, U_{mem} represents the membrane potential, t represents the timestep, and λ represents the leak factor for membrane potential. Meanwhile, Y represents the weighted input of a neuron, w represents the weight at synapse- i , and δ represents the input spike from synapse- i at timestep- t . If the U_{mem} reaches the threshold potential (U_{thr}), then a spike is generated as an output (Z). Otherwise, no spike is generated.

2.2 NAS without Training Approach

In this work, we consider the "NAS without training" approach, as it can quickly find a network that can achieve high accuracy. This approach was originally proposed for ANNs [22], then adopted and modified for SNNs. Its main idea is to perform network evaluation early using a fitness function, hence the performance of network can be evaluated before completing the training phase [22]. For instance, SNASNet [16] leverages the studies in [22] for evaluating the given network through its representation capabilities on diverse samples. Specifically, SNASNet employs the following key steps.

- First, it feeds mini-batch S samples to the network, and monitor its LIF neurons' activity. If the U_{mem} reaches U_{thr} , then the neuron is mapped to 1, otherwise 0. In each layer, this mapping is recorded as binary vector b .
- It computes the Hamming distance $H(b_i, b_j)$ between samples i and j to construct matrix \mathbf{M}_H as shown in Eq. 4. Here, B is the number of neurons in the investigated layer, while γ is the normalization factor to address high sparsity issue from LIF neurons.

$$\mathbf{M}_H = \begin{pmatrix} B - \gamma H(b_1, b_1) & \cdots & B - \gamma H(b_1, b_S) \\ \vdots & \ddots & \vdots \\ B - \gamma H(b_S, b_1) & \cdots & B - \gamma H(b_S, b_S) \end{pmatrix} \quad (4)$$

- Afterward, it calculates the fitness score R of the given architecture candidate using Eq. 5. The highest-scored candidate is then selected for training.

$$R = \log \left(\det \left| \sum_l \mathbf{M}_H^l \right| \right) \quad (5)$$

In this work, we also employ the same evaluation steps for our HASNAS framework, as these steps provide an effective and generic measure for evaluating diverse network architectures.

2.3 NAS with Neural Cell Strategy

The neural cell-based NAS strategy aims at providing a unified benchmark for NAS algorithms [10]. A cell is a directed acyclic graph (DAG) whose edge denotes a specific pre-defined operation. Originally, a cell is designed with 4 nodes with 5 pre-defined operations: *No Connection* (Zeroize), *Skip Connection* (SkipCon), *1x1 Convolution* (1x1Conv), *3x3 Convolution* (3x3Conv), and *3x3 Average Pooling* (3x3AvgPool); the connection between 2 nodes refers to a specific pre-defined operation [10, 16]. The main idea of this strategy is to find the appropriate connection topology and operations inside the cell, as shown in Fig. 4. In this work, we also employ the similar neural Cell-Based strategy for our HASNAS framework, and focus on the feed-forward connection topology as it has been extensively used in the SNN community.

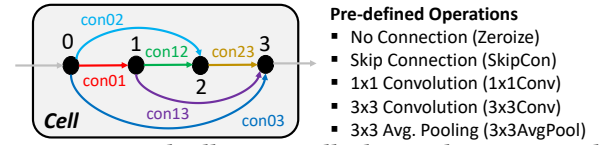


Figure 4: A neural cell is originally designed as a DAG with 4 nodes, whose each connecting edge corresponds to a specific pre-defined operation [10].

2.4 CIM Hardware Architecture

In this work, we consider the CIM hardware platform whose hierarchical architecture is shown in Fig. 5. This CIM design is based on the SpikeFlow architecture from studies in [23].

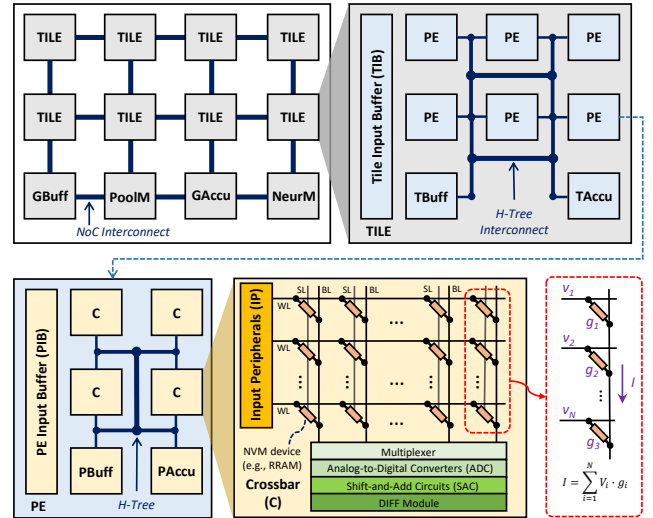


Figure 5: The CIM hardware architecture that is considered in this work. It is based on the SpikeFlow architecture from studies in [23].

At the top level, the CIM architecture consists of tiles for computation, a pooling module (PoolM) for pooling operation, a global buffer (GBuff) for storage, a global accumulator (GAccu) for accumulation operation, and a neuron module (NeurM) for LIF neuron activity. These modules are connected to each other through network-on-chip (NoC) interconnection. Each tile consists of a tile input buffer (TIB), a number of processing elements (PE), a tile buffer (TB), and a tile accumulator (TAccu). Each PE consists of a PE input buffer (PIB), a number of analog crossbars (C), PE buffer

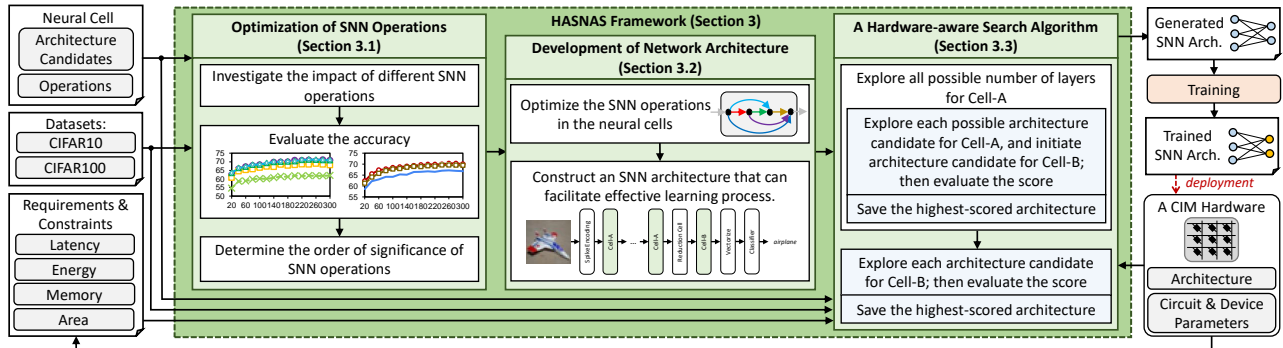


Figure 6: Overview of our HASNAS framework, and its key steps for generating an appropriate SNN architecture that can achieve high accuracy while meeting the given memory, area, latency, and energy consumption constraints; the novel contributions are highlighted in green.

(PBuf), and PE accumulator (PAccu). These modules are connected to each other through H-Tree interconnection. Furthermore, each crossbar consists of input peripherals (IP), RxR non-volatile memory (NVM) device array, multiplexers, analog-to-digital converter (ADC), shift-and-add circuit (SAC), and DIFF module. Here, DIFF module receives the dot-product outputs from SAC, and performs signed multiply-and-accumulate (MAC) operations.

3 THE HASNAS FRAMEWORK

To address the research problem and challenges, we propose a novel HASNAS framework whose design flow is presented in Fig. 6 and its key steps are discussed in the Section 3.1 - Section 3.3, consecutively.

3.1 Optimization of SNN Operations

To construct an efficient SNN architecture that can achieve high accuracy, we have to understand the significance of SNN operations and then select the ones that lead to high accuracy with small memory cost. To do this, we perform an experimental case study with the following scenarios.

- *Scenario-1:* We remove a specific operation from the pre-defined ones (i.e., Zeroize, SkipCon, 1x1Conv, 3x3Conv, and 3x3AvgPool), and then perform NAS to evaluate the impact of the investigated operation on accuracy.
- *Scenario-2:* We investigate the impact of other operations, i.e., 5x5 Convolution (5x5Conv) and 7x7 Convolution (7x7Conv), and then perform NAS to evaluate their impact on accuracy and memory. To do this, the operation that has the role of extracting features (i.e., 3x3Conv) is replaced by the investigated operation. For instance, when 5x5Conv is investigated, the pre-defined operations will consist of Zeroize, SkipCon, 1x1Conv, 5x5Conv, and 3x3AvgPool. The same applies when 7x7Conv is investigated.

Note, all scenarios in this case study consider a Cell-Based network architecture in SNASNet [16] with the CIFAR100 workload. Experimental results are presented in Fig. 7, from which we make the following key observations.

- ① Eliminating Zeroize, 1x1Conv, 3x3AvgPool from the search space do not significantly change the accuracy as compared to the baseline. Hence, these operations can be removed from the search space. If model compression is needed for reducing the memory size, we can keep 3x3AvgPool in the search space. Moreover, it also ensures the connectivity between nodes and between layers.

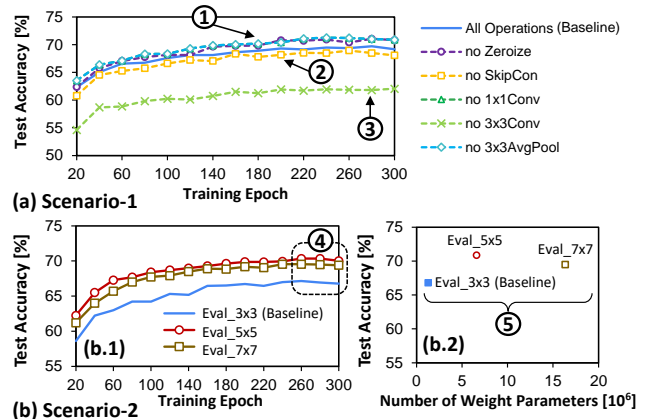


Figure 7: (a) Results of eliminating different operations from the search space of the cell architecture. (b) Results of investigating the impact of 5x5Conv and 7x7Conv operations. Eval_3x3, Eval_5x5, and Eval_7x7 correspond to the accuracy when evaluating the impact of 3x3Conv, 5x5Conv, and 7x7Conv, respectively.

- ② Eliminating SkipCon from the search space slightly reduces the accuracy, as SkipCon is beneficial for providing feature maps from previous layer to preserve important information. Similar observation is also discussed in [6]. Hence, SkipCon should be kept in the search space to maintain the learning quality.
- ③ Eliminating 3x3Conv from the search space significantly degrades accuracy, as the role of 3x3Conv is for extracting important features from input samples. Hence, 3x3Conv should be kept in the search space to maintain the learning quality.
- ④ In general, 5x5Conv and 7x7Conv operations have positive impact on accuracy since larger kernel sizes are capable of extracting more unique input features, which is beneficial for tasks with a large number of classes to distinguish (e.g., CIFAR100).
- ⑤ Despite the benefits on accuracy, larger kernel sizes incur significant memory overheads as compared to the baseline, which usually lead to significant overheads on latency and energy consumption. Hence, these large kernel sizes are not suitable for application use-cases that have stringent memory budgets.

These observations suggest the order of significance of SNN operations from the highest to the lowest in terms of both accuracy and memory cost: (1) 3x3Conv, (2) SkipCon, (3) 3x3AvgPool, then (4) Zeroize, 1x1Conv, 5x5Conv, and 7x7Conv. We leverage this information for enhancing the hardware-aware NAS, so that it can effectively find an SNN architecture that can achieve high accuracy under multiple constraints.

3.2 Development of SNN Architecture

3.2.1 Neural Cell Architecture. Our discussion in Section 3.1 suggest that we can optimize the search space of Cell-Based NAS strategy for improving/maintaining accuracy while keeping the memory footprint low. To do this, we select a few operations that have positive impact on accuracy with low memory cost to be considered in the search space. Specifically, in this work, we consider *SkipCon*, *3x3Conv*, and *3x3AvgPool* operations in the search space, while keeping 4 nodes of DAG in the neural cell.

3.2.2 SNN Macro-Architecture. To improve the applicability of SNN deployments for diverse ML-based applications, we propose an efficient construction/skeleton of SNN macro-architecture; see Fig. 8. The proposed SNN macro-architecture consists of a spike encoding layer, N layer(s) of the Cell-A, a reduction cell, 1 layer of the Cell-B, a vectorize layer, and a classifier. We also employ a non-fixed number of layer for the Cell-A, as it will be determined in the NAS process. This strategy aims to facilitate more variations in the search space to further enhance the learning quality, because a deeper network typically can achieve higher accuracy at the cost of larger memory footprint, as shown by our experimental results in Fig. 9. Furthermore, the Cell-A and the Cell-B are similar as they consider the same kernel size of convolutional operation (3x3Conv), and they differ only in the number of weight filters. The reason is that, later layers (e.g., the Cell-B) typically have more filters than the earlier layers (e.g., the Cell-A), as we need to capture as many combinations of features as possible in the later layers through the increasing number of filters. It is also the reason why we apply multiple layers using the Cell-A, as this strategy incurs a smaller number of weights than applying multiple layers using the Cell-B.

In this manner, our HASNAS framework provides a dynamic search to find a network architecture that has a good trade-off among accuracy, memory, area, latency, and energy consumption.

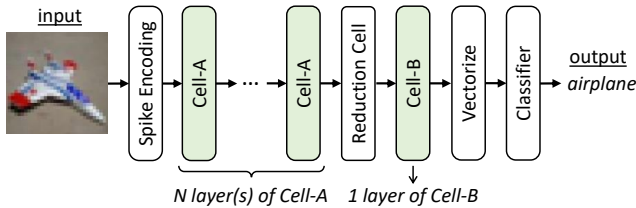


Figure 8: The proposed SNN macro-architecture. It has N layer(s) of the Cell-A and 1 layer of the Cell-B.

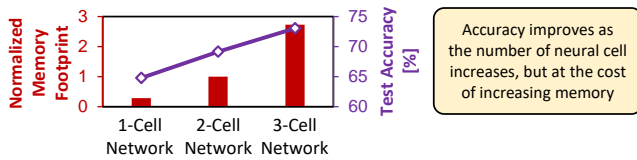


Figure 9: The accuracy vs memory trade-off among the 1-cell, 2-cell, and 3-cell network architectures.

3.3 A Hardware-aware Search Algorithm

To systematically perform NAS while fulfilling multiple design requirements and constraints, we propose a novel hardware-aware search algorithm. Its pseudo-code is presented in Alg. 1.

Algorithm 1 Our Hardware-aware Search Algorithm

```

INPUT: [1] Number of pre-defined iteration for the Cell-A layers ( $N$ );
[2] Number of pre-defined operations in the cell ( $P$ ), with operation codes: SkipCon=0, 3x3Conv=1, and 3x3AvgPool=2;
[3] Cell architectures: Cell-A ( $con\_cellA$ ), Cell-B ( $con\_cellB$ );
[4] Constraints: memory ( $const\_mem$ ), area ( $const\_mem$ ), latency ( $const\_lat$ ), energy consumption ( $const\_eng$ );
[5] Functions: create a cell architecture (create_cell), create a network architecture (create_net), calculate memory (cal_mem), calculate area (cal_area), calculate latency (cal_latency), calculate energy consumption (cal_energy); calculate fitness score (eval);
OUTPUT: Generated an SNN architecture ( $net\_arch$ );
BEGIN
  Initialization:
  1:  $score_h = -1000$ ;
  Process:
  // Search for the Cell-A architecture(s) and layer(s)
  2: for ( $i = 1; i < (N+1); i++$ ) do
  3:   for ( $c01=0; c01 < P; c01++$ ) do
  4:     for ( $c02=0; c02 < P; c02++$ ) do
  5:       for ( $c03=0; c03 < P; c03++$ ) do
  6:         for ( $c12=0; c12 < P; c12++$ ) do
  7:           for ( $c13=0; c13 < P; c13++$ ) do
  8:             for ( $c23=0; c23 < P; c23++$ ) do
  9:                $con\_cellA[i] = create\_cell(c01, c02, c03, c12, c13, c23)$ ;
 10:              if ( $i=1$ ) then
 11:                 $con\_cellB = create\_cell(c01, c02, c03, c12, c13, c23)$ ;
 12:                 $arch = create\_net(con\_cellA, con\_cellB)$ ;
 13:                 $cost\_mem = calc\_mem(arch)$ ;
 14:                if ( $cost\_mem \leq const\_mem$ ) then
 15:                   $score = eval(arch)$ ;
 16:                  if ( $score > score_h$ ) then
 17:                     $score_h = score$ ;
 18:                     $net\_arch = arch$ ;
 19:                     $con\_cellA\_saved = con\_cellA$ ;
 20:                     $con\_cellB\_saved = con\_cellB$ ;
  // Search for the Cell-B architecture
 21: for ( $c01=0; c01 < P; c01++$ ) do
 22:   for ( $c02=0; c02 < P; c02++$ ) do
 23:     for ( $c03=0; c03 < P; c03++$ ) do
 24:       for ( $c12=0; c12 < P; c12++$ ) do
 25:         for ( $c13=0; c13 < P; c13++$ ) do
 26:           for ( $c23=0; c23 < P; c23++$ ) do
 27:              $con\_cellB = create\_cell(c01, c02, c03, c12, c13, c23)$ ;
 28:              $arch = create\_net(con\_cellA\_saved, con\_cellB)$ ;
 29:              $cost\_mem = calc\_memory(arch)$ ;
 30:             if ( $cost\_mem \leq const\_mem$ ) then
 31:                $cost\_area = calc\_area(arch)$ ; // using ELA [23]
 32:               if ( $cost\_area \leq const\_area$ ) then
 33:                  $cost\_lat = calc\_latency(arch)$ ; // using ELA [23]
 34:                 if ( $cost\_lat \leq const\_lat$ ) then
 35:                    $cost\_eng = calc\_energy(arch)$ ; // using ELA [23]
 36:                   if ( $cost\_eng \leq const\_eng$ ) then
 37:                      $score = eval(arch)$ ;
 38:                     if ( $score > score_h$ ) then
 39:                        $score_h = score$ ;
 40:                        $net\_arch = arch$ ;
 41:                        $con\_cellB\_saved = con\_cellB$ ;
 42: return  $net\_arch$ ;
END

```

The key ideas of our hardware-aware search algorithm are discussed in the following.

- Our search policy is that, each cell has an individual search to find its architecture, hence exploring all possible candidates from different combinations of architectures across multiple cells: Cell-A (Alg. 1: line 2-8) and Cell-B (Alg. 1: line 21-26).
- To do this, we first explore possible number of layers for Cell-A (Alg. 1: line 2), as well as possible architectures inside the

Cell-A (Alg. 1: line 3-9). Here, the Cell-B architecture is set the same as Cell-A in the first layer iteration (Alg. 1: line 10-11). Then, we construct the investigated network architecture based on the states of Cell-A(s) and Cell-B (Alg. 1: line 12).

- Afterward, we evaluate the candidate for its memory cost (Alg. 1: line 13-14). If the memory constraint is met, then we continue with the fitness function evaluation (Alg. 1: line 15). If the fitness score is higher than the saved one, then we record the network architecture as a solution candidate (Alg. 1: line 16-20).
- After all layer iterations for Cell-A are finished, we explore possible architectures inside the Cell-B (Alg. 1: line 21-27). Then, we construct the investigated network architecture based on the states of Cell-A(s) and Cell-B (Alg. 1: line 28).
- Afterward, we evaluate the candidate for its memory cost (Alg. 1: line 29-30). If the memory constraint is met, then we continue with evaluation of area, latency, and energy consumption, consecutively (Alg. 1: line 31-36). If all constraints are met, we continue with the fitness function evaluation (Alg. 1: line 37). If the fitness score is higher than the saved one, then we record the network architecture as a solution candidate (Alg. 1: line 38-41).
- After all exploration steps are finished, then we consider the saved network architecture as the solution of the NAS process (Alg. 1: line 42), and this SNN architecture is ready for training.

Note, in this search algorithm, we perform memory evaluation by leveraging the number weight parameters. Meanwhile, we perform area, latency, and energy evaluations using an energy-latency-area (ELA) simulator from studies in [23], while considering the Spike-Flow CIM hardware architecture with real measurements-based values for RRAM device technology.

4 EVALUATION METHODOLOGY

To evaluate our HASNAS framework, we build an experimental setup and tools flow as shown in Fig. 10, while considering the same evaluation settings as widely used in the SNN community [26, 29–32, 37]. Meanwhile, the design requirements and constraints considered in the evaluation are presented in Table 1. For brevity, we refer the HASNAS with 2×10^6 (2M), 4×10^6 (4M), 6×10^6 (6M), and 8×10^6 (8M) memory constraints to as HASNAS_2M, HASNAS_4M, HASNAS_6M, and HASNAS_8M respectively.

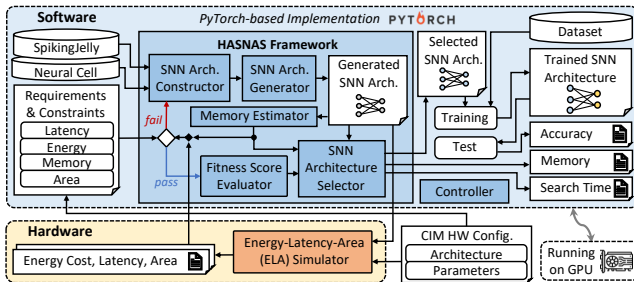


Figure 10: The experimental setup and tools flow.

Software-level Evaluation: To evaluate and validate our proposed techniques, we develop a PyTorch-based implementation using the SpikingJelly library [11], then run it on the Nvidia GeForce RTX 4090 GPU machine which has 24GB GDDR6X memory. We perform network training using the surrogate gradient learning [25, 45]

up to 300 training epochs, while gradually evaluating the test accuracy during the training to observe the learning curve of the investigated SNN architecture. For the workloads, we consider the CIFAR10 and CIFAR100 datasets. For the comparison partner, we reproduce the state-of-the-art Cell-Based NAS without training SNASNet [16] using its default settings, i.e., 2 neural cells, 5 predefined operations, and 5000x iterations of random search. Outputs from the software-level evaluation include the information of accuracy, memory, and searching time of the investigated network architecture.

Hardware-level Evaluation: To evaluate area, latency, and energy consumption when running the SNN architecture on the RRAM-based CIM platform, we employ the state-of-the-art energy-latency-area (ELA) simulator from the work of [23]. The detailed circuit and device parameters of the CIM platform considered in the ELA simulator for evaluating area, latency, and energy consumption are presented in Table 2.

Table 1: Design requirements and constraints considered in the evaluation methodology.

Metric	Value
Memory Footprint	2M, 4M, 6M, and 8M of weights
Area	100 mm^2
Latency	400 ms
Energy Consumption	120 μJ

Table 2: The circuit and device parameters considered in the ELA simulator; adapted from studies in [23].

Circuit Parameters	
NoC Topology	Mesh
NoC Width	32bits
Clock Frequency	250MHz
Crossbar Count-per-PE	9
PE Count-per-Tile	8
Multiplexer Size	8
Sizes of GBuff, TBuf, PBuf	20KB, 10KB, 5KB
Sizes of TIB and PIB	50KB, 30KB
V_{DD}	0.9V
V_{read}	0.1V
Precision of Crossbar ADC	4bits
Column Parasitic Resistance	5 Ω

RRAM Device Parameters [13]	
Bits/Cell	1
R_{on}, R_{off}	20k Ω , 200k Ω
Write Variation	0.1

5 EXPERIMENTAL RESULTS AND DISCUSSION

5.1 Maintaining High Accuracy

Fig. 11(a) and Fig. 11(b) present the experimental results for the accuracy for CIFAR10 and CIFAR100, respectively. The state-of-the-art SNASNet achieves 92.58% of accuracy for CIFAR10 and 66.78% of accuracy for CIFAR100. The network generation in SNASNet simply relies on the number of search iteration with random search and the fitness score. Meanwhile, HASNAS_2M achieves 91.28% of accuracy for CIFAR10 and 63.25% for CIFAR100, HASNAS_4M achieves 91.87% of accuracy for CIFAR10 and 64.67% for CIFAR100, HASNAS_6M achieves 91.67% of accuracy for CIFAR10 and 65.52% for CIFAR100, HASNAS_8M achieves 91.87% of accuracy for CIFAR10 and 65.52% for CIFAR100. These results indicate that, our HASNAS can maintain the high accuracy as compared to the state-of-the-art across all training epochs. The reasons are the following: (1) HASNAS only employs SNN operations that have high significance

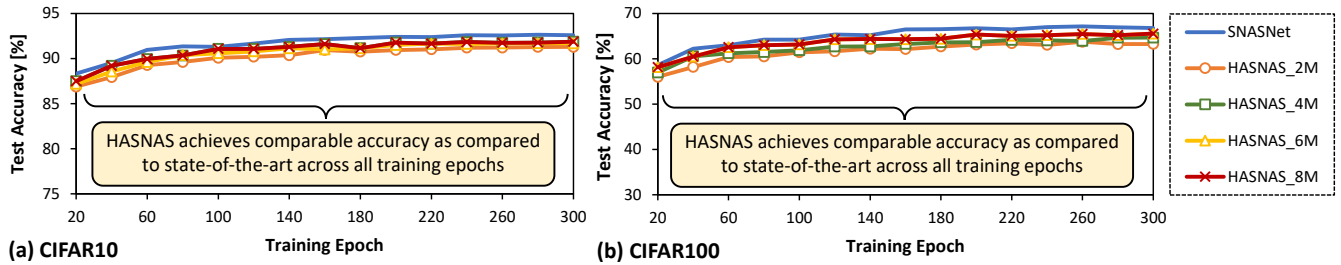


Figure 11: Experimental results of the test accuracy achieved by SNASNet and HASNAS across training epochs for (a) CIFAR10 and (b) CIFAR100 workloads.

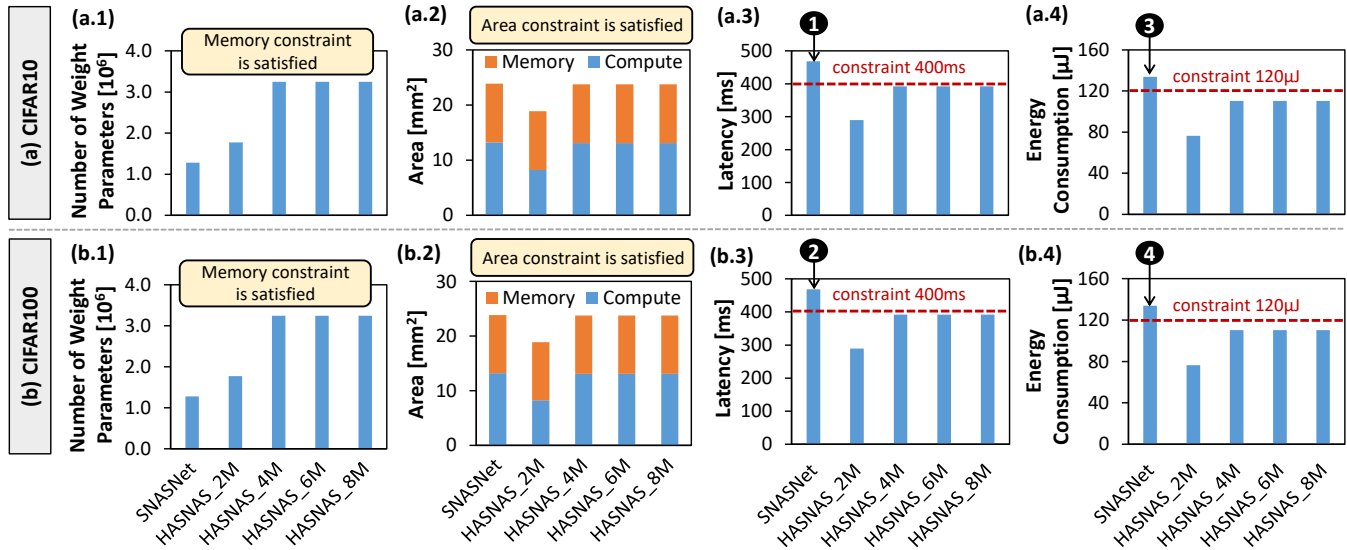


Figure 12: Experimental results of the memory footprint, hardware area, latency, and energy consumption achieved by SNASNet and HASNAS for (a) CIFAR10 and (b) CIFAR100 workloads.

and positive impact on the accuracy, and (2) HASNAS constructs the network by systematically stacking neural cell layer one-by-one, while exploring the appropriate architecture for each neural cell, thereby ensuring effective search toward the desired network architecture.

These results indicate that, *our HASNAS framework successfully maintains the accuracy high and comparable to the state-of-the-art, despite the fact that it has to consider multiple constraints at once during its NAS process, which is not trivial.*

5.2 Ensuring Hardware-aware SNN Generation

Fig. 12 presents the experimental results for hardware-related evaluation considering CIFAR10 and CIFAR100, including memory footprint, hardware area, latency, and energy consumption.

Number of Weight Parameters (Memory Footprint): Results for memory footprint are shown in Fig. 12(a.1) for CIFAR10 and Fig. 12(b.1) for CIFAR100. For the CIFAR10 case, SNASNet generates a network that has 1.28M weight parameters. Since SNASNet does not include the memory constraint in its NAS process, the number of weight parameters of the generated network is not under control during its NAS process. Meanwhile, our HASNAS techniques ensure that the generated network always fulfills the memory constraint, as it includes the information of memory budget in its NAS process. For instance, HASNAS_2M generates a network that has

1.77M weight parameters, which satisfies the memory constraint of 2M parameters. Furthermore, HASNAS_4M, HASNAS_6M, and HASNAS_8M generate networks that have 3.25M weight parameters, which satisfy the corresponding memory constraints, i.e., 4M, 6M, and 8M weight parameters, respectively. We also observe that similar experimental results are obtained for the CIFAR100 case. Here, SNASNet generates a network that has 1.28M weight parameters. Then, our HASNAS_2M generates a network that has 1.77M weight parameters, while HASNAS_4M, HASNAS_6M, and HASNAS_8M generate networks that have 3.25M weight parameters. The reason is that, NAS processes in SNASNet and HASNAS find cell architectures that incur similar numbers of weight parameters to the CIFAR10 case, despite having different cell architectures.

These results indicate that, *our HASNAS framework successfully generates a network architecture that satisfies the given memory constraint, thereby making it possible to store all weight parameters of a network in the memory of underlying hardware platforms.*

Hardware Area: Results for hardware are shown in Fig. 12(a.2) for CIFAR10 and Fig. 12(b.2) for CIFAR100. For the CIFAR10 case, SNASNet generates a network that occupies $23.9mm^2$ area (55% compute and 45% memory parts). Since SNASNet does not include the area constraint in its NAS process, the hardware area of the generated network is not under control during its NAS process. Meanwhile, our HASNAS techniques ensure that the generated

network fulfills the area constraint, as it includes the information of area budget in its NAS process. For instance, HASNAS_2M generates a network that occupies $18.9mm^2$ area (44% compute and 56% memory parts), while HASNAS_4M, HASNAS_6M, and HASNAS_8M generate networks that occupy $23.7mm^2$ area (55% compute and 45% memory parts), thereby meeting the $100mm^2$ area budget. We also observe that similar experimental results are obtained for the CIFAR100 case. Here, SNASNet generates a network that occupies $23.9mm^2$ area. Then, our HASNAS_2M generates a network that occupies $18.9mm^2$ area, while HASNAS_4M, HASNAS_6M, and HASNAS_8M generate networks that occupy $23.7mm^2$ area. The reason is that, the similar numbers of weight parameters from the generated networks by SNASNet and HASNAS for the CIFAR10 and CIFAR100 cases lead to the similar area for hardware implementation.

These results indicate that, *our HASNAS framework successfully generates a network architecture that satisfies the given area constraint, thereby making it possible to develop the corresponding hardware implementation within a custom area budget.*

Processing Latency: Results for processing latency are shown in Fig. 12(a.3) for CIFAR10 and Fig. 12(b.3) for CIFAR100. For both the CIFAR10 and CIFAR100 cases, SNASNet generates networks that require $469ms^2$ processing latency when run on the CIM hardware, which is 17.15% slower than the latency constraint; see label-❶ and label-❷ in Fig. 12. The reason is that, SNASNet does not consider the latency constraint in its NAS process, hence the processing latency the generated network cannot be controlled during its NAS process. Meanwhile, our HASNAS techniques ensure that the generated network meets the latency constraint, by incorporating the information of latency constraint and hardware characteristics in its NAS process. For instance, our HASNAS_2M generates a network that can be run on the CIM hardware in $290ms$ for SNN inference, which is 27.58% faster than the constraint. Meanwhile, our HASNAS_4M, HASNAS_6M, and HASNAS_8M generate networks that can be run on the CIM hardware in $392ms$, which is still within the constraints' envelope.

These results show that, *our HASNAS framework successfully generates a network architecture that satisfies the given latency constraint, which is crucial for SNN deployments on latency-sensitive application use-cases.*

Energy Consumption: Results for energy consumption are shown in Fig. 12(a.4) for CIFAR10 and Fig. 12(b.4) for CIFAR100. For both the CIFAR10 and CIFAR100 cases, SNASNet generates networks that incur $134\mu J$ energy consumption, which is 11.51% worse than the energy constraint; see label-❸ and label-❹ in Fig. 12. The reason is that, SNASNet does not consider the energy constraint in its NAS process, hence the processing energy the generated network cannot be estimated and managed during its NAS process. Meanwhile, our HASNAS techniques ensure that the generated network meets the energy constraint, by incorporating the information of energy constraint and hardware characteristics in its NAS process. For instance, our HASNAS_2M generates a network that incurs $76.4\mu J$, which is 36.37% lower than the constraint. Meanwhile, our HASNAS_4M, HASNAS_6M, and HASNAS_8M generate networks that incur $110\mu J$, which is still within the constraints' envelope.

These results indicate that, *our HASNAS framework successfully generates a network architecture that satisfies the energy constraint,*

thereby enabling a better power/energy management for diverse application use-cases, especially the ones powered by portable batteries.

5.3 Searching Time Speed-Up

Fig. 13(a) and Fig. 13(b) present the experimental results for the searching time for CIFAR10 and CIFAR100, respectively. In both cases of workloads (CIFAR10 and CIFAR100), our HASNAS offers significant speed-up for the searching time as compared to the state-of-the-art. For the CIFAR10 case, HASNAS improves the searching time by 11.1x, 5.39x, 5.27x, and 4.92x for HASNAS_2M, HASNAS_4M, HASNAS_6M, and HASNAS_8M, respectively. Meanwhile, for the CIFAR100 case, HASNAS improves the searching time by 7.4x, 3.72x, 3.66x, and 3.66x for HASNAS_2M, HASNAS_4M, HASNAS_6M, and HASNAS_8M, respectively. The reason is that, our HASNAS employs a fewer SNN operations, minimizes redundant architecture candidates to evaluate, incorporates multiple constraints into the search process, hence leading to a smaller search space and a faster searching time as compared to the state-of-the-art. These results demonstrate that, *our HASNAS can quickly generate network architectures that can maintain high accuracy, while satisfying multiple constraints.*

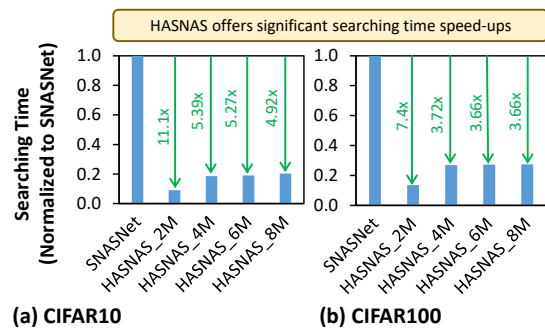


Figure 13: Experimental results of the searching time achieved by SNASNet and HASNAS for (a) CIFAR10 and (b) CIFAR100 workloads.

6 CONCLUSION

We propose the HASNAS framework to find an appropriate SNN architecture that can obtain high accuracy under multiple design requirements and constraints (i.e., memory, area, latency, and energy consumption). It is achieved by optimizing SNN operations, developing an efficient SNN architecture, and designing a hardware-aware search algorithm that incorporates the given constraints in the NAS process. Our HASNAS maintains the high accuracy comparable to state-of-the-art, while fulfilling all constraints. For CIFAR10 and CIFAR100 workloads with constraints of 4M parameters of memory, $100mm^2$ of area, $400ms$ of latency, and $120\mu J$ of energy consumption, our HASNAS can quickly find an appropriate SNN by up to 11x speed-up than the state-of-the-art; where the state-of-the-art cannot meet the latency and energy constraints. In this manner, our HASNAS framework enables the efficient design automation for developing neuromorphic CIM systems for diverse applications.

ACKNOWLEDGMENTS

This work was partially supported by the NYUAD Center for Artificial Intelligence and Robotics (CAIR), funded by Tamkeen under the NYUAD Research Institute Award CG010.

REFERENCES

- [1] Filipp Akopyan et al. 2015. TrueNorth: Design and Tool Flow of a 65 mW 1 Million Neuron Programmable Neurosynaptic Chip. *IEEE Transactions on Computer-Aided Design of Integrated Circuits and Systems (TCAD)* 34, 10 (Oct 2015).
- [2] Jason M. Allred and Kaushik Roy. 2020. Controlled Forgetting: Targeted Stimulation and Dopaminergic Plasticity Modulation for Unsupervised Lifelong Learning in Spiking Neural Networks. *Frontiers in Neuroscience* 14 (2020), 7.
- [3] Aayush Ankit, Abhronil Sengupta, Priyadarshini Panda, and Kaushik Roy. 2017. Resparc: A reconfigurable and energy-efficient architecture with memristive crossbars for deep spiking neural networks. In *54th Annual Design Automation Conference (DAC)*. 1–6.
- [4] Chiara Bartolozzi, Giacomo Indiveri, and Elisa Donati. 2022. Embodied neuro-morphic intelligence. *Nature communications* 13, 1 (2022), 1024.
- [5] Arindam Basu, Lei Deng, Charlotte Frenkel, and Xueyong Zhang. 2022. Spiking Neural Network Integrated Circuits: A Review of Trends and Future Directions. In *IEEE Custom Integrated Circuits Conference (CICC)*. 1–8.
- [6] Hadjer Benmezziane, Amine Ziad Ounnoughene, Imane Hamzaoui, and Younes Bouhadjar. 2023. Skip Connections in Spiking Neural Networks: An Analysis of Their Effect on Network Training. In *IPDPSW Workshop Scalable Deep Learning over Parallel And Distributed Infrastructures (ScaDL)*.
- [7] Kaiwei Che, Zhaokun Zhou, Zhengyu Ma, Wei Fang, Yanqi Chen, Shuaijie Shen, Li Yuan, and Yonghong Tian. 2023. Auto-Spikformer: Spikformer Architecture Search. *arXiv preprint arXiv:2306.00807* (2023).
- [8] Loic Cordone, Benoit Miramond, and Philippe Thierion. 2022. Object Detection with Spiking Neural Networks on Automotive Event Data. In *Int. Joint Conf. on Neural Networks (IJCNN)*. 1–8.
- [9] Mike Davies et al. 2018. Loihi: A Neuromorphic Manycore Processor with On-Chip Learning. *IEEE Micro* 38, 1 (Jan 2018), 82–99.
- [10] Xuanyi Dong and Yi Yang. 2020. NAS-Bench-201: Extending the Scope of Reproducible Neural Architecture Search. In *International Conference on Learning Representations (ICLR)*.
- [11] Wei Fang, Yanqi Chen, Jianhao Ding, Zhaofei Yu, Timothée Masquelier, Ding Chen, Liwei Huang, Huihui Zhou, Guoqi Li, and Yonghong Tian. 2023. Spiking-Jelly: An Open-Source Machine Learning Infrastructure Platform for Spike-based Intelligence. *Science Advances* 9, 40 (2023).
- [12] Wei Fang, Zhaofei Yu, Yanqi Chen, Timothée Masquelier, Tiejun Huang, and Yonghong Tian. 2021. Incorporating Learnable Membrane Time Constant to Enhance Learning of Spiking Neural Networks. In *IEEE/CVF Int. Conf. on Computer Vision (ICCV)*. 2661–2671.
- [13] Basma Hajri, Hassen Aziza, Mohammad M Mansour, and Ali Chehab. 2019. RRAM device models: A comparative analysis with experimental validation. *IEEE Access* 7 (2019), 168963–168980.
- [14] E. M. Izhikevich. 2003. Simple model of spiking neurons. *IEEE Transactions on Neural Networks (TNN)* 14, 6 (Nov. 2003), 1569–1572.
- [15] E. M. Izhikevich. 2004. Which model to use for cortical spiking neurons? *IEEE Transactions on Neural Networks (TNN)* 15, 5 (Sep. 2004), 1063–1070.
- [16] Youngeun Kim, Yuhang Li, Hyoungseob Park, Yeshwanth Venkatesha, and Priyadarshini Panda. 2022. Neural Architecture Search for Spiking Neural Networks. In *European Conference on Computer Vision (ECCV)*. Springer, 36–56.
- [17] Sarada Krithivasan, Sanchari Sen, Swagath Venkataramani, and Anand Raghunathan. 2019. Dynamic Spike Bundling for Energy-Efficient Spiking Neural Networks. In *IEEE/ACM International Symposium on Low Power Electronics and Design (ISLPED)*. 1–6.
- [18] Chankyu Lee, Syed Shakib Sarwar, Priyadarshini Panda, Gopalakrishnan Sriniwasan, and Kaushik Roy. 2020. Enabling Spike-based Backpropagation for Training Deep Neural Network Architectures. *Frontiers in Neuroscience (FNINS)* (2020), 119.
- [19] Qianhui Liu, Jiaqi Yan, Malu Zhang, Gang Pan, and Haizhou Li. 2024. LitE-SNN: Designing Lightweight and Efficient Spiking Neural Network through Spatial-Temporal Compressive Network Search and Joint Optimization. *arXiv preprint arXiv:2401.14652* (2024).
- [20] Yuling Luo, Qiang Fu, Juntao Xie, Yunbai Qin, Guopei Wu, Junxiu Liu, Frank Jiang, Yi Cao, and Xuemei Ding. 2020. EEG-Based Emotion Classification Using Spiking Neural Networks. *IEEE Access* 8 (2020), 46007–46016.
- [21] Wolfgang Maass. 1997. Networks of spiking neurons: The third generation of neural network models. *Neural Networks* 10, 9 (1997), 1659–1671.
- [22] Joe Mellor, Jack Turner, Amos Storkey, and Elliot J Crowley. 2021. Neural Architecture Search without Training. In *International Conference on Machine Learning (ICML)*. 7588–7598.
- [23] Abhishek Moitra, Abhiroop Bhattacharjee, Runcong Kuang, Gokul Krishnan, Yu Cao, and Priyadarshini Panda. 2023. SpikeSim: An End-to-End Compute-in-Memory Hardware Evaluation Tool for Benchmarking Spiking Neural Networks. *IEEE Transactions on Computer-Aided Design of Integrated Circuits and Systems* 42, 11 (2023), 3815–3828. <https://doi.org/10.1109/TCAD.2023.3274918>
- [24] Byunggook Na, Jisoo Mok, Seongsik Park, Dongjin Lee, Hyeokjun Choe, and Sungroh Yoon. 2022. AutoSNN: Towards energy-efficient spiking neural networks. In *International Conference on Machine Learning (ICML)*. 16253–16269.
- [25] Emre O Neftci, Hesham Mostafa, and Friedemann Zenke. 2019. Surrogate gradient learning in spiking neural networks: Bringing the power of gradient-based optimization to spiking neural networks. *IEEE Signal Processing Magazine* 36, 6 (2019), 51–63.
- [26] João D. Nunes, Marcelo Carvalho, Diogo Carneiro, and Jaime S. Cardoso. 2022. Spiking Neural Networks: A Survey. *IEEE Access* 10 (2022).
- [27] Wenxuan Pan, Feifei Zhao, Guobin Shen, Bing Han, and Yi Zeng. 2023. Multi-scale Evolutionary Neural Architecture Search for Deep Spiking Neural Networks. *arXiv preprint arXiv:2304.10749* (2023).
- [28] Michael Pfeiffer and Thomas Pfeil. 2018. Deep Learning With Spiking Neurons: Opportunities and Challenges. *Frontiers in Neuroscience* 12 (2018), 774.
- [29] Rachmad Vidya Wicaksana Putra, Muhammad Abdullah Hanif, and Muhammad Shafique. 2021. ReSpawn: Energy-efficient fault-tolerance for spiking neural networks considering unreliable memories. In *2021 IEEE/ACM International Conference On Computer Aided Design (ICCAD)*. IEEE, 1–9.
- [30] Rachmad Vidya Wicaksana Putra, Muhammad Abdullah Hanif, and Muhammad Shafique. 2022. EnforceSNN: Enabling resilient and energy-efficient spiking neural network inference considering approximate DRAMs for embedded systems. *Frontiers in Neuroscience (FNINS)* 16 (2022), 937782.
- [31] Rachmad Vidya Wicaksana Putra, Muhammad Abdullah Hanif, and Muhammad Shafique. 2022. SoftSNN: Low-Cost Fault Tolerance for Spiking Neural Network Accelerators under Soft Errors. In *ACM/IEEE Design Automation Conference (DAC)*. 151–156.
- [32] Rachmad Vidya Wicaksana Putra, Muhammad Abdullah Hanif, and Muhammad Shafique. 2023. RescueSNN: Enabling Reliable Executions on Spiking Neural Network Accelerators under Permanent Faults. *Frontiers in Neuroscience (FNINS)* 17 (2023), 1159440.
- [33] Rachmad Vidya Wicaksana Putra, Alberto Marchisio, Fakhreddine Zayer, Jorge Dias, and Muhammad Shafique. 2024. Embodied Neuromorphic Artificial Intelligence for Robotics: Perspectives, Challenges, and Research Development Stack. *arXiv preprint arXiv:2404.03325* (2024).
- [34] Rachmad Vidya Wicaksana Putra and Muhammad Shafique. 2020. FSpiNN: An Optimization Framework for Memory-Efficient and Energy-Efficient Spiking Neural Networks. *IEEE Transactions on Computer-Aided Design of Integrated Circuits and Systems (TCAD)* 39, 11 (2020), 3601–3613.
- [35] Rachmad Vidya Wicaksana Putra and Muhammad Shafique. 2021. SpikeDyn: A Framework for Energy-Efficient Spiking Neural Networks with Continual and Unsupervised Learning Capabilities in Dynamic Environments. In *58th ACM/IEEE Design Automation Conference (DAC)*. 1057–1062.
- [36] Rachmad Vidya Wicaksana Putra and Muhammad Shafique. 2022. lpSpikeCon: Enabling Low-Precision Spiking Neural Network Processing for Efficient Unsupervised Continual Learning on Autonomous Agents. In *Int. Joint Conf. on Neural Networks (IJCNN)*. 1–8.
- [37] Rachmad Vidya Wicaksana Putra and Muhammad Shafique. 2023. TopSpark: A Timestep Optimization Methodology for Energy-Efficient Spiking Neural Networks on Autonomous Mobile Agents. In *2023 IEEE/RSJ International Conf. on Intelligent Robots and Systems (IROS)*. 3561–3567.
- [38] Rachmad Vidya Wicaksana Putra and Muhammad Shafique. 2024. SpikeNAS: A Fast Memory-Aware Neural Architecture Search Framework for Spiking Neural Network Systems. *arXiv preprint arXiv:2402.11322* (2024).
- [39] Nitin Rathi, Priyadarshini Panda, and Kaushik Roy. 2019. STDP-Based Pruning of Connections and Weight Quantization in Spiking Neural Networks for Energy-Efficient Recognition. *IEEE Transactions on Computer-Aided Design of Integrated Circuits and Systems (TCAD)* 38, 4 (April 2019), 668–677.
- [40] Arnab Roy, Swagath Venkataramani, Neel Gala, Sanchari Sen, Kamakoti Veezhinathan, and Anand Raghunathan. 2017. A Programmable Event-driven Architecture for Evaluating Spiking Neural Networks. In *IEEE/ACM International Symposium on Low Power Electronics and Design (ISLPED)*. 1–6.
- [41] Catherine D Schuman, Thomas E Potok, Robert M Patton, J Douglass Birdwell, Mark E Dean, Garrett S Rose, and James S Plank. 2017. A survey of neuromorphic computing and neural networks in hardware. *arXiv preprint arXiv:1705.06963* (2017).
- [42] Sanchari Sen, Swagath Venkataramani, and Anand Raghunathan. 2017. Approximate Computing for Spiking Neural Networks. In *Design, Automation Test in Europe Conference and Exhibition (DATE)*, 2017. 193–198.
- [43] Amirhossein Tavanaei, Masoud Ghodrati, Saeed Reza Kheradpisheh, Timothée Masquelier, and Anthony Maida. 2019. Deep learning in spiking neural networks. *Neural Networks* 111 (2019), 47–63.
- [44] Ziqing Wang, Qidong Zhao, Jinku Cui, Xu Liu, and Dongkuan Xu. 2024. Autost: Training-Free Neural Architecture Search For Spiking Transformers. In *IEEE International Conference on Acoustics, Speech and Signal Processing (ICASSP)*. IEEE, 3455–3459.
- [45] Yujie Wu, Lei Deng, Guoqi Li, Jun Zhu, and Luping Shi. 2018. Spatio-temporal backpropagation for training high-performance spiking neural networks. *Frontiers in Neuroscience* 12 (2018), 331.
- [46] Yujie Wu, Lei Deng, Guoqi Li, Jun Zhu, Yuan Xie, and Luping Shi. 2019. Direct Training for Spiking Neural Networks: Faster, Larger, Better. In *AAAI Conference on Artificial Intelligence (AAAI)*, Vol. 33. 1311–1318.
- [47] Jiaqi Yan, Qianhui Liu, Malu Zhang, Lang Feng, De Ma, Haizhou Li, and Gang Pan. 2024. Efficient spiking neural network design via neural architecture search. *Neural Networks* (2024), 106172.
- [48] Hanle Zheng, Yujie Wu, Lei Deng, Yifan Hu, and Guoqi Li. 2021. Going Deeper with Directly-trained Larger Spiking Neural Networks. In *AAAI Conference on Artificial Intelligence (AAAI)*, Vol. 35. 11062–11070.